Cardiac Creatine Kinase Metabolite Compartments Revealed by NMR Magnetization Transfer Spectroscopy and Subcellular Fractionation

F. Joubert,[‡] I. Vrezas,[§] P. Mateo,[‡] B. Gillet,[||] J.-C. Beloeil,[||] S. Soboll,[§] and J. A. Hoerter*,[‡]

Institut National de la Santé et de la Recherche Médicale U-446, Cardiologie Cellulaire et Moléculaire, Université Paris-Sud, Chatenay Malabry, France, Résonance Magnétique Nucléaire Biologique, ICSN, Centre National de la Recherche Scientifique, Gif-sur-Yvette, France, and Institut für Physiologische Chemie I, Universität Düsseldorf, Düsseldorf, Germany

Received July 20, 2000; Revised Manuscript Received December 6, 2000

ABSTRACT: In the perfused rat heart NMR inversion transfer revealed the existence of a compartment of ATP not exchanging through creatine kinase (CK), as demonstated by an apparent discrepancy between the forward (F_f) and reverse (F_r) CK flux if this compartment was neglected in the analysis [Joubert et al. (2000) *Biophys. J. 79*, 1−13]. To localize this compartment, CK fluxes were measured by inversion of PCr (inv-PCr) or γATP (inv-ATP), and the distribution of metabolites between mitochondria and cytosol was studied by subcellular fractionation. Physiological conditions were designed to modify the concentration and distribution of CK metabolites (control, adenylate depletion, inhibition of respiration, KCl arrest). Depending on cardiac activity, mitochondrial ATP (mito-ATP) assessed by fractionation varied from 11% to 30% of total ATP. In addition, the apparent flux discrepancy increased together with mito-ATP (F_f/F_r ranged from 0.85 to 0.50 in inv-PCr and from 1.13 to 1.88 in inv-ATP). Under conditions masking the influence of the ATP−P_i exchange on CK flux, the ATP compartment could be directly quantified by the apparent flux discrepancy; its size was similar to that of mito-ATP measured by fractionation. Thus NMR inversion technique is a potential tool to assess metabolite compartmentation in the whole organ.

Creatine kinase (CK)[1] catalyzes the reversible exchange of high-energy phosphate:

$$PCr^{2-} + MgADP^{-} + H^{+} \underset{F_r}{\overset{F_f}{\rightleftharpoons}} Cr + MgATP^{2-}$$

The role of this enzyme in muscle cells has been widely described. The cytosolic CK reaction, functioning at equilibrium, could serve as a spatial and temporal energy buffer to maintain an adequate ATP/ADP ratio in the cells. Besides, the specific localization of CK isoenzymes in the vicinity of myofibrillar and sarcoplasmic reticular ATPases (MM-CK) and of the adenine translocator (mitochondrial CK, mito-CK), has been recognized to play a key role in the function of the subcellular organelles. Although the role of the bound isoforms has been well evidenced in skinned fibers (for review see ref *1*), an experimental approach is still missing to show how these various intracellular compartments interact in the cardiac cell to ensure the continuous balance of energy supply, transfer, and utilization.

^{31}P NMR magnetization transfer techniques have been widely used to measure CK unidirectional fluxes in the myocardium (for review see Table 1 in ref *2*). Since the heart is in steady state, the global forward F_f(PCr→ATP) and reverse F_r(ATP→PCr) fluxes should be equal. However, the simple two-site model, which assumes the cell to be a homogeneous solution, has been recognized as an oversimplification of the cardiac CK exchanges since F_f and F_r were often found to be unequal by saturation transfer measurements (*3*−*5*). The observed flux discrepancy was proposed to result either from the subcellular compartmentalization of substrates or enzymes (*6*−*8*) or from the exchange of ATP with other phosphorus species such as inorganic phosphate, P_i (*5*, *9*). Recently, we showed that both ATP compartmentation and ATP exchange with P_i contribute to the apparent myocardial flux discrepancy (*2*). Indeed, in an in vitro CK system, the full time analysis of an inversion of PCr (inv-PCr) or of γATP (inv-ATP) could independently reveal the presence of an ATP compartment not involved in exchange with PCr. In the beating control rat heart, this is consistent with the existence of an ATP compartment representing about 20% of total ATP.

Here we postulate that this ATP is localized in the mitochondria. Indeed, depending on mitochondrial activity and work, a nonnegligible fraction of metabolites is known to be sequestered in the mitochondria (*10*−*12*). Several physiological conditions were designed to modify CK

* Address correspondence to this author at U-446 INSERM, Cardiologie Cellulaire et Moléculaire, Faculté de Pharmacie, 5 rue J. B. Clément, 92296 Chatenay-Malabry, France. Tel: 33 1 46835759. Fax: 33 1 46835475. E-mail: jacqueline.hoerter@cep.u-psud.fr.

[‡] Université Paris-Sud.

[§] Centre National de la Recherche Scientifique.

[||] Universität Düsseldorf.

[1] Abbreviations: CK, creatine kinase (adenosine 5′-triphosphate−creatine phosphotransferase, EC 2.7.3.2); NMR, nuclear magnetic resonance; F_f, forward flux; F_r, reverse flux; inv-PCr, inversion of PCr magnetization; inv-ATP, inversion of ATP magnetization; sat-P_i, continuous saturation of inorganic phosphate magnetization; mito-CK, mitochondrial CK; 2DG, 2-deoxy-D-glucose; CN, cyanide; hyp, hypoxia.

10.1021/bi001695j CCC: $20.00
Published on Web 01/26/2001

metabolite concentrations and their subcellular distribution in the perfused rat heart. In conditions of adenylate depletion by 2-deoxy-D-glucose (2DG), inhibition of respiration (by cyanide or hypoxia), and systolic arrest (by high KCl), the modifications of forward CK flux have been previously documented by saturation transfer measurement (*4*, *13*, *14*). Both F_f and F_r were measured by inversion transfer of PCr or γATP in the absence and the presence of a continuous saturation of P_i magnetization (sat-P_i). Sat-P_i has been suggested to mask the influence of P_i-ATP exchange on CK flux determination (*15*). The analysis of data with a two-site exchange model revealed an apparent flux discrepancy related to heart activity. The analysis of this apparent flux discrepancy in the various physiological conditions allowed us to quantify an ATP compartment whose size is compatible with that of mitochondrial ATP measured in the same hearts by nonpolar fractionation.

EXPERIMENTAL PROCEDURES

Physiology. Animal experimentation was performed in accordance with the American Heart Association's position statement on research animal usage. Hearts of Wistar male rats (350−450 g) were perfused by the Langendorff technique at a constant flow. A latex balloon inserted in the left ventricle (LV) was inflated to isovolumic conditions of work and allowed recording of contractile parameters as previously described (*13*). The HEPES-buffered perfusate contains sodium acetate, 10 mM, as the oxidative substrate to minimize the activity of glycolysis. Contractility was characterized by the mean coronary pressure (CP), LV systolic (LVP), end diastolic pressure (EDP), heart spontaneous frequency, and rate pressure product (RPP in 10^4 mmHg·beats·min^{-1}). For each heart the oxygen consumption (Q_{O_2}) was inferred from the relationship between contractility and Q_{O_2} as previously described (*13*).

Besides the control group ($n = 15$), four experimental conditions were designed to change the ATP synthesis or utilization and/or the distribution of metabolites in the subcellular compartments. Depletion of cytosolic ATP and PCr was achieved by 15 min of perfusion with 2-deoxy-D-glucose (2DG, 1 mM) in the presence of 4 IU·L^{-1} insulin (Actrapid Novo). To prevent 2DG6P dephosphorylation upon removal of 2DG and thus the maintainenance of a new ATP and PCr steady state, a low concentration of 2DG (0.075 mM) was continuously infused (*13*) (group 2DG, $n = 15$). Suppression of systolic activity by KCl, 20 mM, was performed to decrease ATP utilization (group KCl, $n = 13$). ATP synthesis was partially inhibited by hypoxia (group hyp = 30% of O_2 content, $n = 10$) or by a low cyanide concentration (group CN, [sodium cyanide] = 0.15 mM, $n = 13$). Glycogen was depleted in four additional CN hearts to minimize the possible interference of glycolytic ATP synthesis with CK flux (*16*). Prior to cyanide inhibition, a 25 min infusion of isoproterenol (Sigma, 8×10^{-9} M) followed by a 15 min recovery was used to deplete 80% of the glycogen stores (*17*).

NMR. (1) NMR Protocols. ^{31}P NMR spectra were acquired at 161.93 MHz on a INOVA Varian wide bore magnet in a 20 mm diameter tube as previously described (*2*). Control spectra were obtained with an 80° pulse angle, 4K data point acquisition, a spectral width of 10000 Hz, and a line broadening of 20 Hz. Fully relaxed spectra (repetition time 10 s) were acquired before and after each inversion experiment. Selective inversion of either PCr (inv-PCr) or γATP (inv-ATP) was achieved by a sinc pulse of 15 ms, followed by a variable delay (0−10 s) before the sampling pulse and a 10 s delay for complete relaxation, and required 24 scans (4 scans cycling 6 times through the whole protocol). Inv-PCr was additionally performed with a continuous saturation of P_i resonance to mask the contribution of ATP−P_i exchange in 25 hearts. In all groups the heart was considered to be in quasi steady state; even during inhibition of ATP synthesis the change in metabolite contents was 3 orders of magnitude slower than the velocity of CK flux (*13*).

(2) Analysis of NMR Data. Both pseudo-first-order rate constants k_f and k_r (and fluxes) can be measured simultaneously by inverting either PCr or γATP, a decisive advantage over saturation transfer protocols. For both inversion protocols, the full time analysis of the return to equilibrium of the inverted and noninverted species after different times of mixing is described in the two-site exchange scheme

$$\mathrm{PCr} \underset{k_r}{\overset{k_f}{\rightleftharpoons}} \gamma\mathrm{ATP}$$

by the solutions of McConnell equations:

$$M_{\mathrm{PCr}}(t) = M^{\infty}_{\mathrm{PCr}} + C_1 \exp \lambda_1 t + C_2 \exp \lambda_2 t$$

and

$$M_{\gamma\mathrm{ATP}}(t) = M^{\infty}_{\gamma\mathrm{ATP}} + C_3 \exp \lambda_1 t + C_4 \exp \lambda_2 t$$

where the different constants (C and λ) depend on k_f, k_r, $T_{1\,\mathrm{PCr}}$ and $T_{1\,\gamma\mathrm{ATP}}$ (*18*). The forward F_f and reverse F_r CK fluxes are $F_f = k_f M^{\infty}_{\mathrm{PCr}}$ and $F_r = k_r M^{\infty}_{\mathrm{ATP}}$ (where $M^{\infty}_{\mathrm{PCr}}$ and $M^{\infty}_{\mathrm{ATP}}$ were the mean values of two control spectra obtained before and after inversion protocols expressed in millimolar). The simplification of the system which considers the heart as a homogeneous medium and describes CK in a two-site exchange system (i.e., neglects ATP ⇔ P_i exchange and/or ATP compartmentation) induces errors in flux determination in both saturation (*5*) and inversion transfer protocols. Specifically, in the latter the presence of two ATP pools, one [$\mathrm{ATP}_1 = (1 - f_{\mathrm{ATP}})\mathrm{ATP}_{\mathrm{total}}$] in fast exchange with PCr and a second ($\mathrm{ATP}_2 = f_{\mathrm{ATP}}\mathrm{ATP}_{\mathrm{total}}$) not exchanging (or in slow exchange) with PCr through CK, will result in an incorrect determination of the kinetic parameters and in an apparent flux discrepancy. The apparent F_f/F_r ratio will be below unity in an inv-PCr protocol and above 1 when ATP is inverted (for complete description see ref *2*).

Contrary to PCr, which is only metabolized by CK in the cell, ATP is involved in many other cellular reactions. Due to the high activity of ATP synthesis and hydrolysis in muscle, the ATP−P_i exchange has been recognized as a possible main source of artifact in the determination of CK flux. Considering both an ATP−P_i exchange and an ATP_2 compartment, the exchange system is

$$\mathrm{PCr} \leftrightarrow \gamma\mathrm{ATP}_1 \leftrightarrow \mathrm{P_i} \leftrightarrow \gamma\mathrm{ATP}_2$$

A continuous saturation of P_i (sat-P_i) has been previously suggested to eliminate the effect of $P_i \rightarrow$ ATP exchange on

CK flux measured by saturation transfer (*5*, *15*). In our case the exchange will be reduced to

$$\mathrm{PCr} \underset{k_r}{\overset{k_f}{\rightleftharpoons}} \gamma\mathrm{ATP}_1 \qquad \gamma\mathrm{ATP}_2$$

with new steady-state values of PCr and ATP magnetization under sat-P_i (M^*_{PCr} and $M^*_{\gamma ATP}$). The time evolution of M_{PCr} and $M_{\gamma ATP}$ will be described by

$$\mathrm{d}/\mathrm{d}t\begin{pmatrix} M_{PCr} \\ M_{\gamma ATP_1} \\ M_{\gamma ATP_2} \end{pmatrix} = \begin{pmatrix} -k_{1f} & k_r & 0 \\ k_f & -k_{1r} & 0 \\ 0 & 0 & -1/T_{1\,\gamma ATP_2} \end{pmatrix}\begin{pmatrix} M_{PCr} - M^*_{PCr} \\ M_{\gamma ATP_1} - M^*_{\gamma ATP_1} \\ M_{\gamma ATP_2} - M^*_{\gamma ATP_2} \end{pmatrix}$$

The solutions of this system depend on the type of magnetization transfer protocol: the presence of an ATP compartment will affect the analysis of both PCr and γATP inversion in a different way. Upon inversion of PCr the magnetization of ATP_2 is not initially disturbed and thus constant during the experiment ($\mathrm{d}M_{\gamma ATP_2}/\mathrm{d}t = 0$). The evolution of ATP magnetization, $M_{\gamma ATP}(t)$, depends only on $M_{\gamma ATP_1}$. However, since the sum $M_{\gamma ATP} = M_{\gamma ATP_1} + M_{\gamma ATP_2}$ is experimentally observed, only an apparent reverse flux ($k_r M^*_{\gamma ATP}$) is accessible. The steady state is described by $k_r M^\infty_{PCr} = M^\infty_{\gamma ATP_1}$. Since $M^\infty_{\gamma ATP} = M^\infty_{\gamma ATP_1}/(1 - f_{ATP})$, the ratio F_f/F_r equals $(1 - f_{ATP})$. Therefore, in an inv-PCr protocol with a continuous P_i saturation, correct kinetic parameters will be obtained, and the measured F_f/F_r will directly quantify the fraction of ATP not involved in the CK reaction. Notice that, upon inversion of ATP, f_{ATP} could also been inferred, but the analysis would be more complex since the time evolution of $M_{\gamma ATP}$ is then described by a triple exponential (*2*).

The adjustment of experimental data with theoretical expression was performed using the peak amplitudes and mean line width as previously described (*2*). Inv-ATP and inv-PCr protocols were analyzed separately. To ensure that the flux discrepancy did not result from this procedure, a simultaneous analysis [as generally used in vitro (*18*)] was also performed in control hearts. Because of the time required for a full inversion protocol, both inversions could not be performed on a single heart; thus the analysis had to be done on the averaged time evolution of M_{PCr} and $M_{\gamma ATP}$ in the absence of sat-P_i. This procedure was not further used since it did not allow the deviation from equilibrium to be statistically evaluated and f_{ATP} to be directly quantified. CK flux was expressed in millimolar per second [assuming a total cellular water volume of 2.72 μL·mg of total protein^{-1} (*13*)].

Metabolite Content and Subcellular Distribution. At the end of the NMR experiments all hearts were freeze clamped. Part of the frozen hearts was used to measure ATP, PCr, and creatine contents (in nmol·mg of protein^{-1}) to calculate the metabolite concentrations during magnetization transfer (*19*). Four to five representative hearts of each experimental group were selected to assay the distribution of metabolites between cytosol and mitochondria. Hearts were powdered under liquid nitrogen and freeze-dried (48 h at −40 °C). Tissue fractionation was performed by density gradient centrifugation in nonaqueous media as previously described (*20*). Briefly six to eight fractions were collected from each gradient. In each fraction the activities of marker enzymes for mitochondrial (citrate synthase) and extramitochondrial space (phosphoglycerate kinase) were determined as well as the protein and metabolite contents. From the distribution of marker enzymes in each fraction, protein and metabolite contents were extrapolated to contents in the pure mitochondrial and cytosolic space. Cytosolic concentrations were calculated assuming a volume of 3.5 μL·mg of cytosolic protein^{-1} (*11*).

Free ADP was classically calculated within the hypothesis of CK equilibrium from the NMR measured contents and the apparent equilibrium CK constant (*19*). Besides, cytosolic metabolite concentrations, determined from NMR contents and subcellular fractionation, were used to estimate cytosolic free ADP, ADP_{cyt}, and the affinity of ATP hydrolysis [$A = -\Delta G_0 + RT \ln([ADP_{cyt}][P_{i\,cyt}]/[ATP_{cyt}])$, with $\Delta G_0 = -30.5$ kJ·M^{-1}).

Statistics. All data were expressed as the mean ± SE. Differences between groups were analyzed by the *t*-test or variance analysis and the Student−Newman−Keuls test (significant for $P < 0.05$).

RESULTS

Contractile and Metabolic Characteristics. The initial contractile and metabolic characteristics were similar in each group and were thus pooled. Table 1 also shows the average contractile parameters and metabolite contents of each experimental group during the inversion transfer period. The depletion of cytosolic adenylate by pretreatment with 2DG in the presence of a nonglycolytic substrate induced no significant change in contractility despite a marked reduction in ATP and PCr content (by 35% and 45%, respectively) as previously observed (*13*). Partial inhibition of ATP synthesis by low cyanide concentration or by hypoxia resulted in about 60% decrease in contractility and a rise in EDP (by 20 and 60 mmHg in CN and hyp, respectively). These impairments in contractility were classically associated with a decrease in PCr and ATP, a rise in P_i, but no significant acidosis due to the presence of acetate as previously reported (*14*). In KCl arrested hearts PCr content increased by about 25%.

NMR Measurement of CK Fluxes: Analysis with the Two-Site Model. Both inversion of PCr and γATP protocols were performed in the various experimental groups. In a representative KCl arrested heart, a typical inversion of γATP protocol is shown (Figure 1a) as well as the time evolution of γATP and PCr magnetizations and their fit in a two-site exchange model. The first-order apparent rate constants, k_f and k_r, and the CK fluxes, F_f and F_r, are summarized in Table 2 for the various groups. In inv-PCr, the forward fluxes were similar to control in 2DG and CN groups and decreased significantly in hyp and KCl ($P < 0.05$) as expected from previous determination by saturation transfer protocols (*4*, *13*, *14*). However, unexpectedly in an organ in steady state, high reverse fluxes F_r were found, resulting in apparent discrepancies between F_f and F_r. F_f/F_r values ranged from 0.50 to 0.85 (significantly different from unity in all groups except KCl).

In all groups, inverting the γATP resulted in a correct determination of F_r which was similar to F_f measured by inv-PCr protocol (Table 2). However, high F_f values were at the origin of an apparent flux discrepancy (reaching significance only in the 2DG and control groups: $F_f/F_r =$

Table 1: Contractile and Metabolic Characteristics of the Hearts

		Contractile Performance[a]				
condition	*n*	LVP	frequency	CP	RPP	EDP rise
initial[b]	66	170 ± 4	256 ± 5	61 ± 1	4.3 ± 0.1	
control	15	148 ± 5	273 ± 7	60 ± 1	4.0 ± 0.2	0 ± 1
2DG	15	153 ± 6	269 ± 12	69 ± 4	3.8 ± 0.2	4 ± 2
cyanide	13	118 ± 5[d]	140 ± 10[d]	61 ± 3	1.6 ± 0.1[d]	20 ± 3[d]
hypoxia	10	83 ± 8[d]	180 ± 10[d]	70 ± 2	1.4 ± 0.1[d]	58 ± 4[d]
KCl arrest	13	0	0	68 ± 2	0	0

			Metabolic Characteristics[c]				
condition	pH_i	P_i	PCr	ATP	sum P	ADP	A_{ATP}
initial	7.11 ± 0.01	3.0 ± 0.1	15.0 ± 0.1	7.3 ± 0.2	45.3 ± 0.4	34 ± 1	−59.4 ± 0.3
control	7.08 ± 0.01	2.7 ± 0.2	12.0 ± 0.3	6.9 ± 0.4	39.7 ± 1	48 ± 3	−58.6 ± 0.2
2DG	7.03 ± 0.01[d]	2.1 ± 0.1	6.7 ± 0.3[d]	4.4 ± 0.3[d]	42.2 ± 1.6	76 ± 6[d]	−57.0 ± 0.2
cyanide	7.05 ± 0.01[d]	10.5 ± 0.5[d]	5.3 ± 0.3[d]	5.8 ± 0.3	37.8 ± 0.8	154 ± 15[d]	−51.9 ± 0.3
hypoxia	7.10 ± 0.01	10.6 ± 0.7[d]	7.4 ± 0.4[d]	4.2 ± 0.3[d]	34.5 ± 1.3	70 ± 5[d]	−52.8 ± 0.3
KCl	7.13 ± 0.01[d]	1.6 ± 0.2	15.4 ± 0.3[d]	7.0 ± 0.4	42.4 ± 0.8	30 ± 1	−61.7 ± 0.5

[a] Contractile performance averaged during the inversion transfer period: LVP (left ventricular systolic pressure), CP (coronary pressure), and EDP rise (rise in end diastolic pressure from initial value of 5 mmHg) in mmHg; frequency in beats·min^{-1}; RPP, rate pressure product in 10^4·mmHg·beats·min^{-1}. [b] Initial = contractile and metabolic characteristics averaged during three control spectra taken after 15 min of equilibration; all groups being similar, data were pooled. [c] Metabolic characteristics of the same hearts during inversion (mean values of two fully relaxed spectra acquired just before and just after the inversion transfer period): pH_i, intracellular pH; P_i, inorganic phosphate; PCr, phosphocreatine; ATP; sum P, sum of all NMR visible phosphorus moieties (in mM); free ADP (in μmol), calculated assuming CK equilibrium; A_{ATP}, free energy of ATP hydrolysis (in kJ·M^{-1}). [d] Significantly different from control: $P < 0.05$.

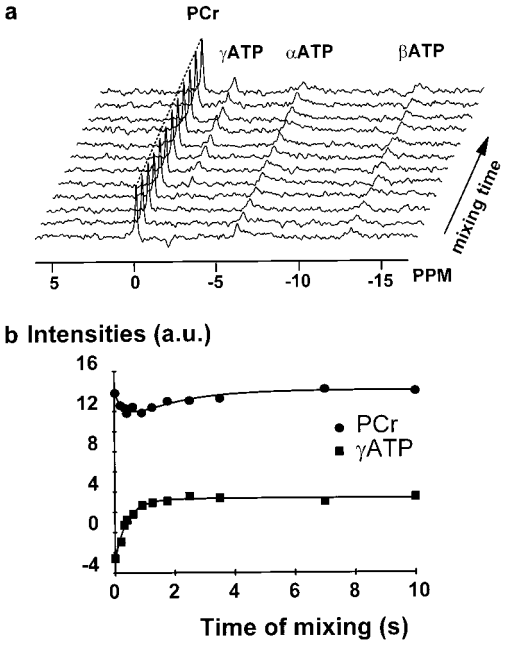

FIGURE 1: Inversion of γATP in a representative heart. (a) Stacked plot of spectra obtained for various times of mixing after the sinc pulse selectively inverting γATP. The dotted line shows the equilibrium magnetization of the noninverted PCr in the absence of inversion. (b) Variation of PCr and γATP magnetization (in arbitrary magnetization units) as a function of the time of mixing and fit in a two-site exchange model.

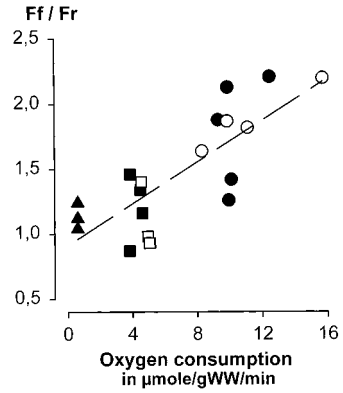

FIGURE 2: Flux discrepancy increased with cardiac activity. F_f/F_r ratios derived from the inv-ATP in the various protocols were related to myocardial oxygen consumption ($r^2 = 0.67$). Physiological conditions: (●) control; (○) 2DG; (■) hypoxia; (□) cyanide; (▲) KCl arrest.

1.88 and 1.73, respectively). The same apparent flux discrepancies as observed here for the various experimental conditions (namely, a forward to reverse flux ratio below unity in an inv-PCr and above unity in inv-ATP protocol) were also observed in vitro, when the existence of an ATP compartment isolated from CK was neglected in the analysis (*2*).

A simultaneous analysis of both inv-ATP and inv-PCr protocols in the two-site exchange model for control hearts confirmed the flux discrepancy; however, it was not systematically performed since this analysis cannot directly quantify the ATP compartment (see Experimental Procedures).

Relation between Flux Discrepancy and Cardiac Activity. A comparison of Tables 1 and 2 suggested that the flux discrepancy increased with myocardial activity. Indeed, F_f/F_r was inversely correlated to oxygen consumption in the inv-PCr protocol (not shown) and positively in inv-ATP (Figure 2 $r^2 = 0.67$). Thus, if this behavior resulted from the presence of an ATP compartment, this compartment should be related to myofibrillar or mitochondrial activity.

Biochemical Estimation of the Intracellular Distribution of Metabolites. Fractionation in Nonaqueous Medium. To identify the localization of this ATP compartment evidenced by NMR, the subcellular distribution of metabolites was measured in some hearts representative of each group by nonpolar fractionation (Table 3). The various physiological conditions altered the distribution of metabolites between cytosolic and mitochondrial compartments. Pretreatment with 2DG, a model depleting the cytosolic adenylate pool but preserving mitochondrial function due to the presence of

Table 2: Parameters of CK Flux Analyzed in the Two-Site Model[a]

	k_f (s^{-1})	k_r (s^{-1})	F_f (mM/s)	F_r (mM/s)	F_f/F_r
inversion of PCr					
control ($n = 5$)	0.60 ± 0.03	2.20 ± 0.24	8.1 ± 0.4	16.0 ± 2.0	0.54 ± 0.05[b]
2DG ($n = 6$)	1.18 ± 0.10	3.10 ± 0.24	6.6 ± 0.7	13.5 ± 1.5	0.50 ± 0.05[b]
cyanide ($n = 5$)	1.31 ± 0.16	1.76 ± 0.15	6.6 ± 0.8	9.8 ± 1.0[c]	0.69 ± 0.06[d]
hypoxia ($n = 3$)	0.33 ± 0.05	1.05 ± 0.24	2.6 ± 0.5[c]	4.2 ± 1.1[c]	0.67 ± 0.08[d]
KCl ($n = 4$)	0.37 ± 0.02	1.00 ± 0.09	5.7 ± 0.1[c]	6.8 ± 0.5[c]	0.85 ± 0.05
inversion of γATP					
control ($n = 5$)	1.01 ± 0.10	1.16 ± 0.06	13.3 ± 1.3	7.8 ± 0.4	1.78 ± 0.17[d]
2DG ($n = 4$)	1.93 ± 0.25	1.52 ± 0.20	12.0 ± 1.3	6.3 ± 0.4[c]	1.88 ± 0.10[d]
cyanide ($n = 4$)	2.16 ± 0.15	1.62 ± 0.07	9.2 ± 0.5[c]	7.4 ± 0.3	1.27 ± 0.10
hypoxia ($n = 4$)	0.55 ± 0.07	0.94 ± 0.08	3.8 ± 0.6[c]	3.2 ± 0.4[c]	1.21 ± 0.11
KCl ($n = 4$)	0.39 ± 0.04	0.84 ± 0.05	6.2 ± 0.6[c]	5.5± 0.4[c]	1.13 ± 0.03

[a] Fluxes were calculated with the relations $F_f = k_f M^{\infty}_{PCr}$ and $F_r = k_f M^{\infty}_{ATP}$, where M^{∞}_{PCr} and M^{∞}_{ATP} (in mM) were the mean values of control spectra (interpulse delay = 10 s) obtained just before and after the inversion transfer. Intrinsic relaxation parameters were similar in all groups: mean values were $T_{1\,\gamma ATP} = 0.7 \pm 0.1$ s and $T_{1\,PCr} = 2.7 \pm 0.3$ s (notice that $T_{1\,PCr}$ could not be reliably measured in the inv-ATP protocol). [b] F_f/F_r significantly different from unity: $P < 0.001$. [c] Significantly different from control: $P < 0.05$. [d] F_f/F_r significantly different from unity: $P < 0.05$.

Table 3: Mitochondrial Metabolites Measured by Nonpolar Fractionation[a]

	protein	ATP	ADP	AMP	Cr	PCr	P_i
control ($n = 5$)	44.2 ± 2.9	22.5 ± 1.9	36.7 ± 2.8	72.3 ± 6.5	30.2 ± 4.9	13.6 ± 2.1	35.6 ± 6.4
2DG ($n = 4$)	40.3 ± 2.5	29.5 ± 5.5	38.8 ± 3.1	81.7 ± 4.5	31.0 ± 4.4	18.1 ± 3.7	53.1 ± 10.2
hypoxia ($n = 4$)	43.5 ± 1.1	15.8 ± 1.5[b]	29.8 ± 3.9	73.2 ± 4.0	50.9 ± 4.4[b]	9.7 ± 2.3	36.9 ± 6.5
cyanide ($n = 4$)	46.0 ± 6.7	16.3 ± 0.8[b]	37.2± 2.4	24.8 ± 4.3[b]	18.0 ± 2.8	6.7 ± 2.9	30.1 ± 2.7
KCl ($n = 5$)	44.7 ± 1.7	11.0± 1.3[b]	39.4 ± 4.1	63.0 ± 8.2	23.8 ± 3.4	5.9 ± 0.4[b]	39.9 ± 4.0

[a] Expressed in % of total metabolites. [b] Significantly different from control: $P < 0.05$.

oxidative substrate, resulted in the highest mitochondrial ATP fraction (≅30% of total ATP vs 23% in control). The mitochondrial ATP fraction was significantly lower than the control, when ATP synthesis was partly inhibited by hyp or CN (15.8% and 16.3% of total ATP) and further decreased to 11% when systolic activity was prevented by high KCl. Similar differences between physiological conditions were observed in the subcellular distribution of PCr and ADP. The size of the PCr compartments ranged from 6% to 18% of total. In the various groups the increase in mitochondrial PCr and ADP concentration was linearly related to that of ATP ($r^2 = 0.79$ and 0.45, respectively; not shown) while AMP and creatine concentrations were independent of ATP.

Comparison of Biochemical and NMR Data. (A) Identification of the ATP Compartment Observed by NMR. The relationship between F_f/F_r observed by NMR and the mitochondrial ATP fraction measured by subcellular fractionation in different physiological conditions is shown in Figure 3a for inv-PCr and in Figure 3b for inv-ATP. The apparent discrepancy between F_f and F_r increased, together with the mitochondrial ATP fraction for both inversion protocols. This is indeed exactly the same behavior as observed when we increased the size of the ATP compartment not involved in CK in vitro (*2*). Thus, mitochondrial ATP could contribute to the apparent flux discrepancy observed in the various experimental conditions in myocardium.

(B) Quantification of the Size of the ATP Compartment by NMR. The influence of the ATP ⇔ P_i exchange on the determination of CK flux is shown by the comparison of flux values obtained in inv-PCr without (Table 2) and with (Table 4) a continuous saturation of P_i. Sat-P_i did not affect F_f determination but modified F_r and thus the ratio F_f/F_r. Thus the ATP compartment f_{ATP} could only be quantified when the influence of the ATP−P_i exchange was masked by sat-P_i. When PCr was inverted, f_{ATP} simply equaled $1 - F_f/F_r$ (Table 4), whereas, in the inv-ATP protocol, f_{ATP} could be inferred from a triple exponential analysis of the data (not shown). Similar values were obtained for f_{ATP} inferred from NMR and the mitochondrial ATP measured by fractionation. In all groups except CN a good correlation was observed between both methods (Figure 4). The 3-fold overestimation of f_{ATP} in CN possibly resulted from contamination by other reactions; it could be related to an increased glycogenolytic activity since, after depletion of glycogen stores (group CN + ISO), f_{ATP} became similar to the fractionation determination.

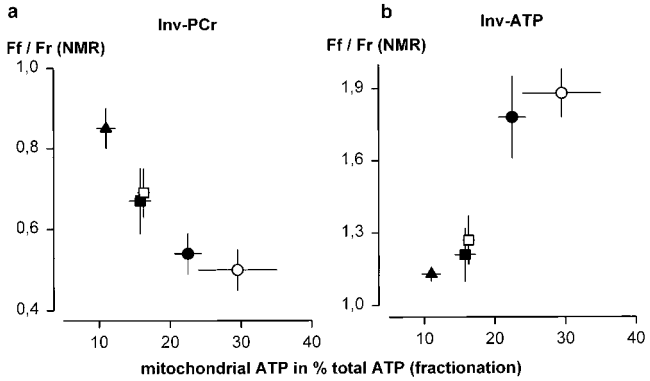

FIGURE 3: Relation between flux discrepancy and mitochondrial ATP: (a) inversion of PCr; (b) inversion of γATP. Same symbols as in Figure 2. Mitochondrial ATP measured by fractionation is expressed in percent of total ATP.

DISCUSSION

When the fluxes of CK were measured by a full time analysis of inversion transfer, significant discrepancies were observed between forward, F_f, and reverse, F_r, CK fluxes in both protocols of inversion of PCr or of γATP, an observa-

Table 4: Parameters of CK Flux in Perfused Hearts Extracted from the Inversion Transfer Protocols with Saturation of P_i[a]

inversion of PCr	F_f (mM/s)	F_r (mM/s)	F_f/F_r	f_{ATP}
control ($n = 5$)	6.9 ± 0.8	8.8 ± 1.1[b]	0.80 ± 0.06[b,c]	0.20 ± 0.06[b]
2DG ($n = 5$)	6.8 ± 0.6	9.7 ± 1.0[b]	0.73 ± 0.07[b,c]	0.27 ± 0.07[b]
cyanide ($n = 4$)	5.8 ± 1.2	12.5 ± 2.8[b]	0.47 ± 0.01[b,c]	0.53 ± 0.01[b]
cyanide + ISO ($n = 3$)	7.1 ± 0.8	9.2 ± 2.1	0.83 ± 0.09	0.17 ± 0.09
hypoxia ($n = 3$)	4.5 ± 1.0	5.4 ± 1.2	0.84 ± 0.03	0.16 ± 0.03
KCl ($n = 5$)	4.5 ± 0.6[d]	4.8 ± 0.8[d]	0.96 ± 0.06	0.04 ± 0.06

[a] Mean $T_{1\,PCr} = 3.3 \pm 0.5$ s and mean $T_{1\,\gamma ATP} = 0.7 \pm 0.1$ s. [b] Significantly different from Table 2 data (protocol without saturation of P_i): $P < 0.05$. [c] F_f/F_r significantly different from unity: $P < 0.05$. [d] Significantly different from control: $P < 0.05$.

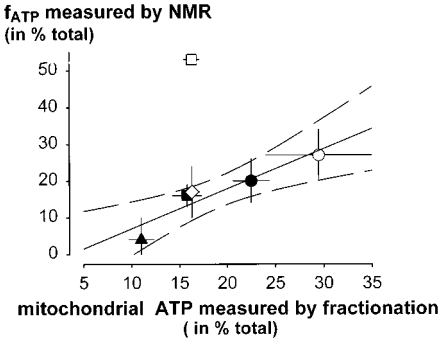

FIGURE 4: Comparison of the size of the ATP compartment inferred from inv-PCr protocols under saturation of P_i and the mitochondrial ATP measured by fractionation. f_{ATP} inferred from NMR was correlated with mitochondrial ATP measured by fractionation. The slope of this relation (plain line and dotted line, 95% confidence interval) was not significantly different from unity ($y = 1.1x - 5$, $r^2 = 0.919$, without cyanide; see Results). Same symbols as in Figure 2 plus (◇) cyanide glycogen depleted.

tion unexpected in an organ in steady state. We previously demonstrated in vitro (*2*) that an apparent flux discrepancy arises from neglecting in the analysis the presence of an ATP compartment not directly exchanging with CK; however, this simple analysis allowed us to directly quantify the fraction of ATP not involved in CK. Here we explored the hypothesis that in myocardium the observed apparent flux discrepancy, which is not expected in an organ in steady state, might also result from the analysis of NMR data in a simplistic model neglecting ATP compartmentation. This analysis can, however, be used to quantify the ATP compartment in the whole heart when the possible influence of the ATP−P_i exchange on CK measurement was masked. In various physiological conditions, this apparent flux discrepancy increased with contractile activity, which led us to postulate that this ATP compartment should be localized at sites of ATP production or utilization. The main finding of this study is that the size of the ATP compartment revealed by NMR was similar to the mitochondrial ATP fraction measured by nonpolar fractionation. Thus a full time analysis of inversion transfer is able to show mitochondrial metabolite compartmentalization in the whole organ.

Measurement of CK Fluxes by NMR. Unidirectional CK flux has mostly been measured by NMR saturation transfer. However, the definite advantage of a full time course analysis of an inversion transfer protocol is the simultaneous measurement of both forward and reverse fluxes. Although inversion protocols have been suggested, as opposed to saturation, not to probe all of the reactions of CK, in particular those implying small pools of metabolites (*21*, *22*), our results (Table 2) indicate that this might not be the case. The F_f fluxes measured by inv-PCr are similar to those previously measured by saturation of γATP under the various physiological conditions (*4*, *13*, *14*). Since the influence of ATP compartmentalization and ATP−P_i exchange are negligible on the determination of F_f, both techniques should probe the same CK flux. This forward flux should address the global CK flux since the mito-CK flux can be measured in intact heart mitochondria (*23*) and all isoforms are NMR visible in transgenic mice with specific isozyme knockout (*24*, *25*).

The insensitivity of CK flux to a change in cardiac performance or PCr and ATP content is beyond the scope of this work and has been discussed previously for the models of 2DG and cyanide (*13*, *14*), whereas the flux decrease in KCl arrested heart is a classical observation (*4*).

Compartmentation of CK Metabolites. The subcellular distribution of metabolites has been assessed in isolated mitochondria by fractionation of isolated cells or whole organ in nonaqueous solvents. When isolating mitochondria or cells from tissue, part of the metabolites are lost from mitochondria; it is therefore difficult to extrapolate from metabolite contents determined in isolated mitochondria to mitochondrial contents in the tissue in situ. In isolated mitochondria maximal adenine nucleotide contents of about 10 nmol·mg of protein^{-1} can be reached by incubation of rat liver or heart mitochondria with ATP and ADP (*26*). Similar values are obtained when mitochondria are isolated in the presence of carboxyatractyloside to inhibit the translocator. The amount makes about 20−30% of total ATP + ADP content in heart and liver tissue. Our mitochondrial ATP + ADP contents obtained by density gradient fractionation of freeze-clamped and lyophilized tissue in nonpolar solvents are in this range for control hearts. Of course, the mitochondrial ATP content is also dependent on the phosphorylation state of adenine nucleotides and mitochondrial function. As observed here for the hypoxic, cyanide, or KCl arrested groups, mitochondrial ATP has been previously shown to decrease to low values in anoxia or upon KCl arrest (*27*−*29*). The highest mitochondrial fraction of ATP was found in 2DG as expected from both the sustained mitochondrial respiration and the decrease in cytosolic ATP (*13*).

Controversy exists about the presence of creatine in the heart mitochondrial matrix. It has been generally assumed that there is neither Cr nor PCr in the mitochondria, since, due to lack of CK in the matrix space, there is no function for these substrates in the matrix compartment. However, previous studies using nonpolar fractionation and isolated mitochondria clearly showed the presence of both Cr and PCr in the mitochondrial matrix (*11*). The presence of Cr in the matrix and its transport has been previously observed by other groups (*12*, *30*) in both normoxia and ischemia. An intracellular Cr compartment has also been detected by radioactive labeling in rat atria or skeletal muscle (*31*, *32*) or by ^{1}H and ^{31}P NMR in isolated perfused rat heart (*33*) and in skeletal muscle (*34*). Since a physiological function for Cr and PCr is not known, the presence of guanidino compounds in the matrix was suggested to result from a slow transport by the adenine nucleotide translocator and thus to be simply a leak in the creatine shuttle (*35*) although other

Table 5: Cytosolic Metabolite Concentrations Estimated with Fractionation Data[a]

condition	*n*	PCr	ATP	Cr	P_i	free ADP	A_{ATP}
control	15	15.0 ± 0.4	7.9 ± 0.4	11.1 ± 0.3	2.4 ± 0.2	41 ± 3	−59.5 ± 0.2
2DG	15	7.1 ± 0.3	4.0 ± 0.2	15.4 ± 0.2	1.3 ± 0.1	59 ± 5[b]	−58.7 ± 0.2
cyanide	13	7.1 ± 0.4	7.0 ± 0.3	22.0 ± 0.4	10.6 ± 0.5	152 ± 14	−62.6 ± 0.5
hypoxia	10	9.2 ± 0.5	4.8 ± 0.4	11.1 ± 0.3	9.2 ± 0.6	44 ± 3[b]	−54.7 ± 0.3
KCl arrest	13	20.4 ± 0.4	8.7 ± 0.5	9.1 ± 0.4	1.3 ± 0.2	30 ± 1	−52.2 ± 0.3

[a] Hypothesis: cytosolic volume = 3.5 μL/mg of cytosolic protein. [b] Significantly different from ADP calculated from the total cellular concentrations (Table 1).

mechanisms such as a recently described mitochondrial Cr transporter could also contribute to the load of the matrix (*36*).

Bioenergetic Implications. The determination of free ADP (and of the related index ATP/ADP, phosphorylation potential, free energy of ATP hydrolysis) is central to the understanding of bioenergetic regulation of mitochondrial respiration and ATPase activity in the whole organ. Free ADP calculation is usually derived from the global metabolite concentrations measured in NMR, assuming that all CK metabolites are visible and involved in CK reaction and that all CK isoforms function at equilibrium as shown in Table 1. Errors can occur, for example, if a compartment of ATP is localized in the mitochondrial matrix and exchanged via translocase slower than the CK turnover. Besides, if the equilibrium of cytosolic CK is widely accepted, respiration drives mito-CK out of equilibrium (*37*). Here we can directly infer the free cytosolic ADP from the cytosolic concentrations of ATP, PCr, and Cr (Table 5). In two experimental conditions out of five (2DG, hyp), cytosolic free ADP was significantly lower than inferred from total metabolite contents. As a consequence the free energy of ATP hydrolysis was higher when derived from cytosolic than from total concentrations; this high A_{ATP}, similar to control, could participate in the sustained systolic activity observed in the 2DG model. Thus this suggests that the total cytosolic ADP and the related bioenergetic indices might not be accurately estimated from the total metabolite contents in all physiological or pathological conditions as implicit from the observation that CK does not have access to the total PCr and Cr pool (*32*, *33*).

Interpretation of the Discrepancy between F_f and F_r. Magnetization transfer experiments have often been used to discuss CK equilibrium in the whole heart. If consistent data on the forward CK flux have been measured, a large range of values has been reported in the literature for the reverse flux (for review of the literature, see Table 1 in ref *2*). The main problem in the interpretation of a magnetization transfer experiment in vivo arises from the oversimplification of a highly organized cellular system: in other words, the interpretation of data is always model dependent. The use of a two-site model to analyze the data (considering the myocardium as a homogeneous solution and neglecting the influence of the exchange of ATP with other species) is clearly inadequate to describe myocardial CK fluxes.

(i) The Assumption of the ATP−P_i Exchange Is Not Sufficient To Account for the Apparent Discrepancy between Fluxes. The presence of an ATP−P_i exchange has been suggested to explain the apparent discrepancy between both F_f and F_r fluxes in saturation transfer (*5*, *9*) although others have questioned its importance (*7*, *22*). The flux discrepancy previously observed in the perfused heart in protocols of saturation was abolished when the influence of the ATP−P_i exchange on CK flux was masked by a continuous saturation of P_i (*5*). By contrast, masking this exchange was insufficient to account for the flux discrepancy observed in myocardium in vivo (*7*) as in our study. The reason for the discrepancy with the data of Ugurbil (*5*) is not obvious but might be related to our longer interpulse delay allowing full relaxation of all species, the type of magnetization transfer protocol, or the absence of glucose in our protocol. The influence of ATP−P_i exchange was also questioned on theoretical grounds; simulation of its influence (from values derived from oxygen consumption measurement) is not expected to have such an influence on CK flux (*2*, *3*, *22*). In our inversion PCr protocol, saturation of P_i indeed significantly influenced F_r measurement (as shown by comparison of Tables 2 and 4). However, it was insufficient to totally account for the flux discrepancies observed in conditions of high contractile activity.

ATP exchange through other enzymatic reactions has also been considered as a potential pitfall in CK flux determination. ATP ↔ P_i through glyceraldehyde 3-phosphodehydrogenase (*22*) should be minimized in our protocol due to the absence of glycolytic substrate. Concerning the ATP−ADP exchange through adenylate kinase (AK), its contribution could not be evidenced in the normoxic myocardium in vivo (*21*). However, in skeletal muscle ^{18}O labeling revealed that the contribution of AK to energy exchange increased upon inhibition of CK flux (*38*); AK flux could also increase in myocardium when CK flux was impaired (i.e., in hyp and KCl arrested hearts). Although we did not specifically invert βATP to probe the transfer of magnetization to ADP, we never observed in any experimental group a significant magnetization transfer to βATP upon inversion of γATP (and βADP).

(ii) The Assumption of the ATP Compartmentalization. A nonnegligible fraction of metabolite is known to be sequestered in mitochondria (*10*−*12*). The presence of an ATP compartment has early been suggested to potentially interfere with NMR saturation transfer flux measurements (*39*) although its visibility, its potentiality to be magnetically perturbed, and its exchange with PCr have been questioned (*5*, *7*, *8*, *21*). Such an ATP compartment was suggested to account for the flux discrepancy when observed (*6*, *21*), but its influence was never directly experimentally assessed. Here we used the potency of a full time analysis of the inversion transfer to show that an NMR visible ATP compartment can be accurately quantified. The coherence of the NMR and biochemical determination suggests that this ATP compartment is localized in mitochondria and increases in size with contractile performance. This simple hypothesis of ATP compartmentalization was sufficient to account for the apparent flux discrepancy observed by inversion transfer

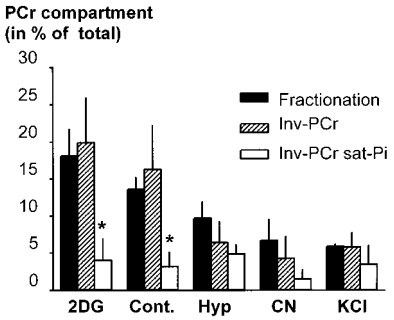

FIGURE 5: Comparison of mitochondrial PCr measured by fractionation and the size of the PCr compartment inferred from inv-PCr protocols with and without sat-P_i. An asterisk indicates a significant difference between NMR and fractionation ($p < 0.05$).

under saturation of P_i resonance. Because matrix ATP does not participate in CK reaction, the return to equilibrium of this pool is not affected by inv-PCr. In terms of NMR this ATP behaves independently of CK although it is in physiological exchange with cytosolic ATP as previously discussed (*2*). There is thus no contradiction between the isolation of ATP by the NMR procedure and the fact that up to 90% of cellular ATP is ultimately labeled in a skeletal muscle when net phosphoryl transfer flux is measured by ^{18}O exchange kinetics (*40*). This mitochondrial ATP compartment is obviously part of the whole heart energy circuit. We believe that the simplistic model of analysis developed here is a useful tool to approach metabolite compartmentation in the whole beating heart but cannot be used to gain information on the communication between metabolic pools (see below).

(iii) Additional Hypothesis of PCr Compartmentalization. Table 4 also reveals the existence of a mitochondrial compartmentalization of PCr. In an inv-PCr protocol, a PCr compartment (PCr_2) would induce additional errors on k_f (but not on F_f) and on reverse flux F_r and thus increase the discrepancy between fluxes in a two-site scheme analysis [$F_f/F_r \cong (1 - f_{ATP})(1 - f_{PCr})$]. The time evolution of PCr would be described by

$$M_{PCr}(t) = M^{\infty}_{PCr} + C_1 \exp \lambda_1 t + C_2 \exp \lambda_2 t + [M_{PCr_2}(0) - M^{\infty}_{PCr_2}] \exp[-(t/T_{1\ PCr_2})]$$

and the discrimination of ATP and PCr compartments thus requires a triple exponential analysis of the data. Such an analysis of the inv-PCr with sat-P_i did not significantly alter the size of the ATP compartment (not shown) and revealed a small PCr compartment (below 5% of total for all experimental conditions; Figure 5). This implies either that mitochondrial PCr measured by fractionation was too small to be observable by NMR or that most of the PCr was perturbed by sat-P_i. We assume the latter. Indeed, in the absence of P_i saturation the size of the NMR-detected PCr compartment was similar to that measured by fractionation (Figure 5). Although this quantification is not rigorous due to contamination by ATP−P_i exchange, it suggests that part of mitochondrial PCr could be affected by sat-P_i; PCr localized in the intermembrane space (ims), together with mito-CK, could be a good candidate because both matrix and ims metabolites are quantified by fractionation as the mitochondrial compartment (*11*). Indeed sat-P_i should mainly affect mitochondrial metabolites when glycolytic ATP production is negligible (due to acetate utilization this should be the case here except for cyanide or hypoxic conditions). Due to the transfer of magnetic perturbation from P_i through ATP synthase and translocase, mito-CK could thus be an indirect target of sat-P_i.

This information on mito-CK together with MM bound and cytosolic fluxes is indeed included in the global flux measurement obtained by inversion protocols without sat-P_i. The analysis of only one experiment of magnetization transfer cannot support such a complexity, except by making numerous assumptions on the size of the metabolic pool involved, their relaxation properties, and the volume of the compartments. Estimations of mito-CK flux in the whole heart have indeed been proposed on the basis of modeling of NMR data obtained by saturating γATP (*8*, *41*). Preliminary work (*42*) suggests that a combined analysis of both inversion experiments in the presence and absence of P_i saturation together with knowledge of the subcellular metabolite distribution might be an experimental strategy to bring precise information on subcellular CK fluxes. In addition, this will directly allow the evaluation of the various models of energy transfer.

ACKNOWLEDGMENT

We thank J. L. Mazet for stimulating discussions, P. Lechene for the programs of analysis, C. Ducrocq and S. Gründel for contribution to the fractionation analysis, E. Boehm for correction of the manuscript, and R. Fischmeister for continuous support.

REFERENCES

1. Saks, V. A., Ventura-Clapier, R., and Aliev, M. K. (1996) *Biochim. Biophys. Acta 1274*, 81−88.
2. Joubert, F., Gillet, B., Mazet, J.-L., Mateo, P., Beloeil, J.-C., and Hoerter, J. A. (2000) *Biophys. J. 79*, 1−13.
3. Matthews, P. M., Bland, J. L., Gadian, D. G., and Radda, G. K. (1982) *Biochim. Biophys. Acta 721*, 312−320.
4. Bittl, J. A., and Ingwall, J. S. (1985) *J. Biol. Chem. 260*, 3512−3517.
5. Ugurbil, K., Petein, M. A., Maiden, R., Michurski, S. P., and From, A. H. L. (1986) *Biochemistry 25*, 100−108.
6. Nunnally, R. L., and Hollis, D. P. (1979) *Biochemistry 18*, 3642−3646.
7. Koretsky, A. P., Wang, S., Klein, M. P., James, T. L., and Weiner, M. W. (1986) *Biochemistry 25*, 77−84.
8. Zahler, R., Bittl, J. A., and Ingwall, J. S. (1987) *Biophys. J. 51*, 883−893.
9. Spencer, R. G., Balschi, J. A., Leigh, J. S., and Ingwall, J. S. (1988) *Biophys. J. 54*, 921−929.
10. Geisbuhler, T., Altschuld, R. A., Trewyn, R. W., Ansel, A. Z., Lamka, K., and Brierley, G. P. (1984) *Circ. Res. 54*, 536−546.
11. Soboll, S., Conrad, A., Keller, M., and Hebisch, S. (1992) *Biochim. Biophys. Acta 1110*, 27−32.
12. Altschuld, R. A., Merola, A. J., and Brierley, G. P. (1975) *J. Mol. Cell. Cardiol. 7*, 451−462.
13. Stepanov, V. P., Mateo, P., Gillet, B., Beloeil, J.-C., and Hoerter, J. A. (1997) *Am. J. Physiol. 273*, C1397−C1408.
14. Mateo, P., Stepanov, V., Gillet, B., Beloeil, J.-C., and Hoerter, J. A. (1999) *Am. J. Physiol. 277*, H308−H317.
15. Ugurbil, K. (1985) *J. Magn. Reson. 64*, 207−219.
16. Kingsley-Hickman, P., Sako, E. Y., Mohanakrishnan, P., Robitaille, P. M. L., From, A. H. L., Foker, J. E., and Ugurbil, K. (1987) *Biochemistry 26*, 7501−7510.
17. Cross, H. R., Opie, L. H., Radda, G. K., and Clarke, K. (1996) *Circ. Res. 78*, 482−491.

18. Led, J. J., and Gesmar, H. (1982) *J. Magn. Reson. 49*, 444−463.
19. Hoerter, J. A., Lauer, C., Vassort, G., and Guéron, M. (1988) *Am. J. Physiol. 255*, C192−C201.
20. Soboll, S., Elbers, R., and Heldt, H. W. (1979) *Methods Enzymol. 56*, 201−206.
21. Koretsky, A. P., Basus, V. J., James, T. L., Klein, M. P., and Weiner, M. W. (1985) *Magn. Reson. Med. 2*, 586−594.
22. Brindle, K. M. (1988) *Prog. NMR Spectrosc. 20*, 257−293.
23. Jahnke, D., Gruwel, M. L. H., and Soboll, S. (1998) *Biochim. Biophys. Acta 1365*, 503−512.
24. Van Dorsten, F. A., Nederhoff, M. G. J., Nicolay, K., and Van Echteld, C. J. A. (1998) *Am. J. Physiol. 275*, 1191−1199.
25. Saupe, K. W., Spindler, M., Hopkins, J. C. A., Shen, W., and Ingwall, J. S. (2000) *J. Biol. Chem. 275*, 19742−19746.
26. Austin, J., and Aprille, J. R. (1984) *J. Biol. Chem. 259*, 154−160.
27. Asimakis, G. K., and Conti, V. R. (1984) *J. Mol. Cell. Cardiol. 16*, 439−447.
28. Kauppinen, R. A., Hitunen, K., and Hassinen, I. E. (1980) *FEBS Lett. 112*, 273−276.
29. Hütter, J. F., Alves, C., and Soboll, S. (1990) *Biochim. Biophys. Acta 1016*, 244−252.
30. Lipskaya, T. Y., and Goloveshkina, V. G. (1975) *Biokhimiya 40*, 942−950 [translation: Plenum Publishing Corp., New York (1976) *10011*, 805−811.
31. Savabi, F. (1988) *Proc. Natl. Acad. Sci. U.S.A. 85*, 7476−7480.
32. Hochachka, P. W., and Mossey, M. K. P. (1998) *Am. J. Physiol. 274*, R868−R872.
33. Unitt, J. F., Schrader, J., Brunotte, F., Radda, G. K., and Seymour, A. M. (1992) *Biochim. Biophys. Acta 1133*, 115−120.
34. Kruiskamp, M. J., VanVliet, G., and Nicolay, K. (2000) *Magn. Reson. Med. 43*, 657−664.
35. Soboll, S., et al. (1994) *Mol. Cell. Biochem. 133/134*, 105−113.
36. Walzel, B., Straumann, N., Hornemann, T., Magyar, J., Kay, L., Kristiansen, S., Richter, E. A., and Wallimann, T. (2000) *Eur. J. Med. Res. 5* (Suppl. 1), 28−29.
37. Saks, V. A., Kuznetsov, A. V., Kupriyanov, V. V., Miceli, M. V., and Jacobus, W. E. (1985) *J. Biol. Chem. 260*, 7757−7764.
38. Dzeja, P. P., Zeleznikar, R. J., and Goldberg, N. N. (1996) *J. Biol. Chem. 271*, 12847−12851.
39. Meyer, R. A., Kushmerick, M. J., and Brown, T. R. (1982) *Am. J. Physiol. 242*, C1−C11.
40. Zeleznikar, R. J., and Goldberg, N. D. (1991) *J. Biol. Chem. 266*, 15110−15119.
41. Aliev, M. K., and Saks, V. A. (1997) *Biophys. J. 73*, 428−445.
42. Joubert, F., Mazet, J.-L., Vrezas, I., Mateo, P., Gillet, B., Beloeil, J.-C., Soboll, S., and Hoerter J. A. (2000) in *Animating the cellular map* (Hofmeyer, J. H. S., Rohwer, J. M., and Snoep, J. L., Eds.) pp 107−112, Stellenbosch University Press, South Africa.

BI001695J